NASA Technical Memorandum 58214

High Temperature Electrolytic Recovery of Oxygen from Gaseous Effluents from the Carbo-chlorination of Lunar Anorthite and the Hydrogenation of Ilmenite: A Theoretical Study

Thomas E. Erstfeld

Lockheed Electronics Company, Inc.

Richard J. Williams

Lyndon B. Johnson Space Center
Houston, Texas

NASA
National Aeronautics and Space Administration

Scientific and Technical Information Office

1979

NASA Technical Memorandum 58214

High Temperature Electrolytic Recovery of Oxygen from Gaseous Effluents from the Carbo-chlorination of Lunar Anorthite and the Hydrogenation of Ilmenite: A Theoretical Study

Thomas E. Erstfeld and Richard J. Williams

April 1979

National Aeronautics and
Space Administration

Lyndon B. Johnson Space Center
Houston, Texas

CONTENTS

SUMMARY

The effluent gases which would result from the reaction of chlorine and carbon with lunar anorthite (carbo-chlorination) and of hydrogen with lunar ilmenite have been calculated. These thermodynamic calculations include the effects of all volatile species which are known to be present in lunar materials. The only gaseous species with a mole fraction greater than 10^{-5} are CO, CO_2, H_2O, N_2, P_4O_{10}, SO_2, SO_3, and He+Ne for the former reaction and H_2, H_2O, CO, CO_2, CH_4, N_2, P_4O_6, H_2S, and He+Ne for the latter. Results indicate that the gaseous products of carbo-chlorination are essentially a mixture of CO_2 and CO, and those of hydrogenation are essentially a mixture of H_2O and H_2. The theoretical analyses of these gases following their electrolytic reduction (with removal of the oxygen) indicate that the aforementioned impurities do not build-up in the system. The currents and voltages associated with such electrolyses have also been calculated for three different ceramic electrolytes. The results indicate that reduction can effectively be performed by this method, and that an yttria stabilized zirconia ceramic will be the most effective one to use.

INTRODUCTION

Some future space activities require for their realization the construction of large structures in space. The largest and best defined of these possible activities is the solar power satellite, for which large quantities of silicon, silica, aluminum, and iron are necessary. For propulsion and life-support large quantities of oxygen are also needed. It has been suggested that lunar material might be a raw material from which metals and oxygen could be extracted for use in near earth space.

The most recent study of chemical extraction techniques is that of Rao and co-workers[1] in which they detailed the extraction of aluminum from anorthite ($CaAl_2Si_2O_8$) by a carbo-chlorination process. Briefly, this process involves the reaction of carbon and chlorine with anorthite; at 1000K, they predicted this reaction would be represented by

$$CaAl_2Si_2O_8 + 8C + 8Cl_2 \rightarrow CaCl_2 + 2AlCl_3 + 2SiCl_4 + 8CO \ . \qquad (1)$$

Aluminum is obtained by electrolyzing $AlCl_3$, and silicon and oxygen are recovered by subsequent chemical and physical processes. Rao et al.[1] also developed a similar process for the recovery of iron and titanium from ilmenite ($FeTiO_3$). However, if only iron recovery is desired, a much simpler process may be constructed on the basis of the reaction of hydrogen with ilmenite. At 1500K, this reaction is

$$FeTiO_3 + H_2 \rightarrow Fe + TiO_2 + H_2O \ . \qquad (2)$$

---

[1] D.B. Rao, U.V. Choudary, T.E. Erstfeld, R.J. Williams, Y.A. Chang, "Extraction Processes for the Production of Aluminum, Titanium Iron, Magnesium, and Oxygen from Non-Terrestrial Sources," 1977 NASA-Ames Space Settlements Summer Study. To be published in Space Resources and Space Settlements, NASA SP-428, 1979.

Both processes produce oxygen from that which is chemically bound in the raw material, but it, too, is chemically bound oxygen, i.e. either CO or H_2O. Also, Rao et al.[1] briefly discussed chemical and electrolytic methods for producing molecular oxygen from the effluent gas. One of their suggested oxygen production techniques is electrolysis at high temperatures using ceramic electrolytes.

In this study, it will be assumed that refining techniques based on carbo-chlorination of anorthite or hydrogenation of ilmenite are employed to refine lunar materials and that oxygen is to be recovered from the effluent gases by high temperature electrolysis using solid oxygen electrolyte ceramics. The purpose of this study is to theoretically analyze this proposed high temperature electrolysis of the refining gases in order to estimate potential yields, power requirements, and materials problems. The first step in this analysis is the estimation of the composition of the refining gases and effects of oxygen removal on the bulk composition of and the species present in the gases.

In this context there are several unresolved questions which have not been studied. Specifically,

- Does carbo-chlorination yield the products given in Eq. 1, or are various calcium silicates, aluminum silicates, and/or calcium aluminates formed?
- What is the minimum chlorine pressure necessary for carbo-chlorination? What are the pressures of volatile metal chlorides?
- What is the effect of naturally occurring volatile impurities on the composition of effluent gases from the previously described reactions?
- How will the composition of the effluent gas change as oxygen is removed?

- At what stage of oxygen removal do physical and chemical interactions with the ceramics become possible? What are these interactions?
- What are the potential oxygen yields as a function of electrical and physical parameters of solid electrolyte systems?

In order to answer the first two questions, calculations were performed which involved several possible reactions which could occur during the carbo-chlorination of anorthite, as a function of chlorine pressure. The third and fourth questions were addressed by calculating the compositions of the effluent gases of both carbo-chlorination and hydrogenation, before and after oxygen removal, for the largest possible amounts of natural volatiles. Finally, the voltage required to decompose CO-CO_2 gas mixtures was calculated from thermodynamic tables, from which current, and ultimately, rates of oxygen production have been calculated.

ANALYSIS OF REFINING REACTIONS

Carbo-chlorination

The thermodynamic parameters for the various reactions which could possibly occur during carbo-chlorination of anorthite were calculated from JANAF tables (ref. 1), for the most part. Free energies of formation of the calcium aluminates (not in JANAF) were calculated by combining data from Kelley (ref. 2) and Parker and co-workers (ref. 3). For the reaction,

$$xCa + yAl + zO_2 \rightarrow Ca_xAl_yO_{2z} \ , \qquad (3)$$

the free energy of formation of $Ca_xAl_yO_{2z}$ at temperature T, ΔG_f^T, is equal to:

$$\Delta G_f^T = \Delta H_f^\circ + \int_{298.15}^{T} \Delta C_p dT - T\left(\Delta S_f^\circ + \int_{298.15}^{T} [\Delta C_p/T]dT\right) , \qquad (4)$$

where ΔH_f° and ΔS_f° are the enthalpy and entropy of formation, respectively, for $Ca_xAl_yO_{2z}$ in the standard state, and

$$\Delta C_p = C_p^{Ca_xAl_yO_{2z}} - xC_p^{Ca} - yC_p^{Al} - zC_p^{O_2} , \qquad (5)$$

i.e., the difference in the heat capacities of the products and the reactants. Free energies of formation of anorthite and a few of the metal oxides were obtained from the data of Robie et al. (ref. 4). For the reaction,

$$aA + bB \rightleftarrows cC + dD , \qquad (6)$$

the free energy of reaction, ΔG°, is related to the equilibrium constant, K, as follows:

$$\Delta G^\circ = -RT \ln K , \qquad (7)$$

where R is the gas constant, and T is absolute temperature. The equilibrium constant is related to the activities, a, of the reactants and products (or the fugacities, f, if they be gases) in the following manner:

$$K = \frac{a_C^c \, a_D^d}{a_A^a \, a_B^b} . \qquad (8)$$

Since the solid and liquid reactants and products for carbo-chlorination are in standard states, their activities are unity, so that the equilibrium constant is equal to the ratio of the fugacities of the effluent gases to the fugacities of the influent gases. In Figure 1, one observes that oxygen fugacity and temperature define a particular CO-CO_2 ratio. By assuming that the ratio of the effluent CO-CO_2 gas mixture from carbo-chlorination is at the point of graphite precipitation at any reaction temperature, i.e. the following reaction,

$$2CO \rightleftarrows CO_2 + C \qquad (9)$$

is at equilibrium, Eq. 1 can therefore be written in terms of oxygen fugacity; thus Eq. 1 becomes

$$CaAl_2Si_2O_8 + 8Cl_2 \rightarrow CaCl_2 + 2AlCl_3 + 2SiCl_4 + 4O_2 \; . \qquad (10)$$

The chlorination reactions of the constituent oxides of anorthite,

$$CaO + Cl_2 \rightarrow CaCl_2 + 1/2\ O_2 \; , \qquad (11)$$

$$SiO_2 + 2Cl_2 \rightarrow SiCl_4 + O_2 \; , \qquad (12)$$

and

$$Al_2O_3 + 3Cl_2 \rightarrow 2AlCl_3 + 3/2\ O_2 \qquad (13)$$

have free energies of reaction of -118.4 kJ/mole, + 204.6 kJ/mole, and +293.7 kJ/mole of metal oxide respectively at 1000K. This suggests that the first step of the reaction indicated by Eq. 10 would be the formation of $CaCl_2$, as it is the only chloride whose formation is favored thermodynamically.

Although this may not necessarily be true, the assumption is reasonable, and it serves as a starting point for our analysis of carbo-chlorination. Constant removal of product gases, i.e. not allowing a state of chemical equilibrium to be achieved, will allow for the production of $AlCl_3$ and $SiCl_4$ from their respective oxides in subsequent steps of the reaction, but only if the oxides Al_2O_3 and SiO_2 can be formed during the first step of the reaction. Rather than forming the desired $CaCl_2$, Al_2O_3, and SiO_2 in the first step, it may be that either aluminum silicates are formed in the first step, or that in the second step, $CaCl_2$ will react with the oxides, thereby forming calcium aluminates and/or calcium silicates. Some reactions which could occur are listed in Table I. The first three equations show the various possible first steps for the anorthite reaction. The latter six equations represent possible reactions of $CaCl_2$ with Al_2O_3 or SiO_2.

The nine reactions listed in Table I are by no means exhaustive in such a complex system as carbo-chlorination of anorthite. Several other side reactions are possible; those which are most noticeable are reactions which produce compounds of Cl-O, C-Cl, and C-Cl-O. Calculations from JANAF Tables (ref. 1) indicate that the most thermodynamically stable Cl-O species is ClO, the most stable C-Cl species is CCl_4, and the most stable C-Cl-O species is $COCl_2$. Under our self-imposed conditions (f_{O_2} is at the CO-CO_2 graphite precipitation point, and f_{Cl_2} is at the minimum fugacity necessary to achieve the desired reaction) the fugacities of these species at 1000K are 4.57×10^{-21}, 1.22×10^{-21}, and 1.65×10^{-12}, respectively. For reasons of simplicity in this study, gases whose mole fractions are less than 10^{-5} times that of the total

gas composition have been deleted, because their effects on the system at the macroscopic level should be insignificant. Of course, if one were to greatly increase the f_{O_2} and/or the f_{Cl_2} in the system, then these species may become present at much higher levels and could not be neglected.

The free energy changes for the reactions in Table I were calculated for a temperature of 1000K and total pressure of 10^5 Pa (1 bar). The oxygen fugacity for the first reaction was arbitrarily (compared to the other eight reactions) set equal to the f_{O_2} (6.33×10^{-22}) at 1000K of the CO-CO_2 system's graphite precipitation point, obtained from Figure 1. By combining this f_{O_2} with the equilibrium constant for that reaction (v. Eq. 8), a value for f_{Cl_2} could be determined. This value was used for the f_{Cl_2} in the other eight reactions. The data are given in Table II. A plot of log f_{Cl_2} versus log f_{O_2} is shown in Figure 2. This figure shows that when carbo-chlorination is performed near the CO-CO_2-graphite equilibrium point at 1000K, the desired reaction will occur when f_{Cl_2} is greater than 6.03×10^{-11}. Since all the plots are parallel, any increase in oxygen fugacity followed by a stoichiometric increase in chlorine fugacity will still achieve the desired results.

In a similar set of calculations, the values of f_{Cl_2} were determined for the nine reactions in Table I as a function of temperature. In this case, the value of f_{O_2} was held constant at each temperature, with the value again being set equal to the f_{O_2} at the graphite precipitation point for the CO-CO_2 equilibrium mixtures. The results of the calculations are shown in Table III. A graphical representation of the data is shown in Figure 3. It shows that over this temperature range which would be practical for carbo-chlorination, the desired products ($CaCl_2$, SiO_2, and Al_2O_3) will always be formed.

Values of f_{SiCl_4} and f_{AlCl_3} at 1000K were determined for the reactions represented by Eqs. 12 and 13, as a function of f_{Cl_2}.

Therefore, at the levels of f_{O_2} and f_{Cl_2} which we are considering, none of the effluent species except CO and CO_2 are present at significant levels. At 1000K and 10^5 Pa (1 bar), an equilibrium gas would be 0.636 CO and 0.364 CO_2.

Hydrogenation

The reaction of hydrogen with ilmenite is much simpler to analyze, since only the reaction represented by Eq. 2 occurs. As long as the solid phases $FeTiO_3$, Fe, and TiO_2 are present, the ratio of H_2/H_2O in the effluent gas is fixed at equilibrium, because Eq. 2 is a combination of

$$FeTiO_3 \rightarrow Fe + TiO_2 + 1/2\ O_2 \qquad (14)$$

and

$$H_2 + 1/2\ O_2 \rightarrow H_2O\ . \qquad (15)$$

From the already cited thermodynamic data, we compute that

$$\log(f_{H_2O}/f_{H_2}) = -2126.1/T + 0.6439\ , \qquad (16)$$

over the temperature range of 1000-1500K. Thus, for temperatures in this range, the effluent gases will be mainly H_2. At 1000K, the mole fraction of H_2 would be 0.97 and at 1500K, 0.85 for 10^5 Pa (1 bar) total pressure.

EFFLUENT GAS COMPOSITIONS

The calculations presented above illustrate that for reactions involving pure $CaAl_2Si_2O_8$ and $FeTiO_3$, the effluent gases are almost completely represented

by the simple systems CO-CO_2 and H_2-H_2O, respectively. The electrolysis of such gases is the primary topic of the rest of this report.

In electrolysis of CO_2 the cathode reaction which occurs is

$$CO_2 + 2e^- \rightarrow CO + O^{2-} \quad . \tag{17}$$

The anode reaction is

$$O^{2-} \rightarrow 1/2\ O_2 + 2e^- \quad , \tag{18}$$

which produces an overall net reaction, which is represented by Eq. 19:

$$2\ CO_2 \rightarrow 2\ CO + O_2 \quad . \tag{19}$$

The ceramic electrolyte to be used in such an electrolysis consists of a metal oxide doped with a second metal oxide in which the two metals are of differing valence states. The ceramic contains anion deficiencies. Under the influence of an electric current, the oxide ions, which are produced by the reaction represented by Eq. 17, will migrate through the solid electrolyte and release electrons on the other side, thereby forming oxygen.

Water is electrolyzed in a similar manner:

$$H_2O + 2e^- \rightarrow H_2 + O^{2-} \quad . \tag{20}$$

By combining this half-reaction with that represented by Eq. 18, an overall reaction, shown by Eq. 21, is obtained:

$$2\ H_2O \rightarrow 2\ H_2 + O_2 \quad . \tag{21}$$

Weissbart and co-workers (ref. 5) have pointed out that there is an interaction between the H-O gas and C-O gas systems. They mentioned the following reaction, represented by Eq. 22:

$$H_2 + CO_2 \rightarrow H_2O + CO \ , \qquad (22)$$

and added, "This reaction converts hydrogen into water which, in small amounts, catalyzes both the cathode reaction in the electrolyzer and the carbon monoxide disproportionation reaction." The mechanism of this catalytic process is unclear and should be determined.

Although these electrolysis reactions occur as described above for essentially pure CO-CO_2 and H_2-H_2O gases which would result from the refining of chemically pure $CaAl_2Si_2O_8$ and $FeTiO_3$, the materials to be refined are minerals which contain volatilizable impurities which might significantly affect the effluent gas compositions, particularly as oxygen is removed from the gas by electrolysis.

The worst-possible effluent gas compositions, in terms of the greatest amounts of impurities being present, were calculated from the levels of impurities which would be present in beneficiated lunar anorthite and ilmenite, as determined by Williams and co-workers.[2] These compositions are presented in Table IV. Also included in this table are the amounts of light volatile elements present, which for the most part are due to solar wind bombardment and meteoritic impact of the lunar surface. The quantities of the light

[2]R.J. Williams, D.S. McKay, D. Giles, T.E. Bunch, "Mining and Beneficiation of Lunar Ores," 1977 NASA-Ames Space Settlements Summer Study. To be published in Space Resources and Space Settlements, NASA SP-428, 1979.

volatile elements were calculated from the Handbook of Lunar Materials (ref. 6). The compositions of the effluent gases were determined by "forming" the greatest possible amount of volatile oxides, and then determining the amount of CO or H_2O (depending on whether carbo-chlorination or hydrogenation were being studied) which can be formed from the remaining reactive oxygen. In the case of the anorthite reaction, all oxygen has been assumed to be reactive; however, with ilmenite, only the oxygen combined as FeO has been assumed to be reactive.

Whether the effluent gas produced by the carbo-chlorination reaction would be CO, an equilibrium mixture (0.636 CO and 0.364 CO_2) or a composition between those extremes will depend on process engineering and reaction kinetics. Furthermore, CO disproportionates by the reaction represented by Eq. 9. The equilibria favor CO_2 formation at low temperatures. These relations are illustrated in Figure 1. Consequently, Table V shows the composition of the effluent gas (i.e. species with mole fractions greater than 10^{-5}) from the carbo-chlorination reaction, before and after CO-CO_2 equilibrium has been achieved. Table VI shows the composition of this system, if the CO were disproportionated at low temperature by a catalyst (and carbon had been removed). Table VII shows the equilibrium compositions of the effluent gases from the hydrogenation reaction, at the temperatures of 1000 and 1500K.

A series of calculations was performed with the gas mixtures to determine the gas compositions after 90 and 99% electrolysis in order to achieve an understanding of the greatest-possible amounts of contaminators, which could theoretically be formed. In practice, however,

it is unlikely that such high levels of electrolysis could be achieved. In the case of the CO-CO_2 system, it was assumed that CO will also undergo electrolysis as shown by Eq. 23,

$$CO + 2e^- \rightarrow C + O^{2-} , \qquad (23)$$

and that the carbon formed by this reaction will be removed, so as not to halt electrolysis by its deposition on the electrolyte; however, carbon removal may prove to be difficult in actuality. In all probability, Eq. 23 is a combination of Eqs. 17 and 9, i.e. as CO_2 is electrolyzed, equilibrium will favor its formation from CO. The composition of the CO-CO_2 system following electrolysis is presented in Table VIII. Table IX shows similar figures for the H_2-H_2O system. As stated earlier, these calculations are for a worst-possible amount of impurities. In all likelihood, the effluent gases will be much "cleaner."

In none of the cases does the level of "impurities", with the exception of N_2 in some extreme cases, reach any significant level. None of the species determined to be present is known to interact with the materials from which a solid ceramic electrolyte electrolysis system would be constructed.

The chlorine fugacities associated with carbo-chlorination are very low and, therefore, are not included among the effluent gases of carbo-chlorination of anorthite (v. Table V). However, since a stabilized zirconia electrolyte is one of the promising types of electrolytes for high temperature electrolysis,

the effect of f_{Cl_2} on systems with ZrO_2, represented by Eq. 24, was calculated:

$$ZrO_2 + 2\ Cl_2 \rightarrow ZrCl_4 + O_2\ . \qquad (24)$$

A graphical representation of the results is shown in Figure 4. These results show that formation of $ZrCl_4$ is thermodynamically more favorable than the formation of $AlCl_3$ or $SiCl_4$. Whether a platinum coating on the ceramic electrolyte will inhibit or prevent this undesirable reaction can only be determined experimentally.

Chlorides of platinum (ceramic coating) and gold (cell contacts) are well-known compounds. Above the temperature 790K in the case of AuCl, and 820K in the case of $PtCl_2$, these compounds will dissociate to the metal and chlorine gas (ref. 7). Therefore, the reaction of chlorine with these metals at the higher temperatures where these experiments will be performed is not expected. The higher halides, $AuCl_3$ and $PtCl_4$, dissociate at even lower temperatures to the lower halides and chlorine gas (ref. 7). In addition, the respective melting points of gold and platinum are 1336 and 2042K. Therefore, the reaction of Cl_2 with ZrO_2 is the sole chemical interaction of any significance found by thermodynamic calculations during this study.

ANALYSIS OF ELECTROLYSIS

The free energies of reaction for the reactions represented by the following equations were calculated to determine the voltages which must be

applied to achieve reaction:

$$ZrO_2 \rightarrow Zr + O_2 \quad (25)$$

$$CaO \rightarrow Ca + 1/2\ O_2 \quad (26)$$

$$Y_2O_3 \rightarrow 2\ Y + 3/2\ O_2 \quad (27)$$

$$ThO_2 \rightarrow Th + O_2 \quad (28)$$

$$CO_2 \rightarrow CO + 1/2\ O_2 \quad (29)$$

$$CO \rightarrow C + 1/2\ O_2 \quad (30)$$

and

$$H_2O \rightarrow H_2 + 1/2\ O_2\ . \quad (31)$$

The electromotive force (or emf), E, is related to the free energy in the following manner:

$$\Delta G = -|z|\ FE\ , \quad (32)$$

in which $|z|$ represents the equivalents of electrons being transferred in the preceding reactions, and F is the Faraday constant, 96487 coul/equivalent. The first four reactions describe the decomposition of the ceramic electrolytes, and the latter three describe electrolytic decomposition of the effluent gases of carbo-chlorination and hydrogenation. The results of these calculations performed at various temperatures are given in Table X as determined from Robie et al. (ref. 4). The data are shown graphically in Figure 5. Because of the CO-CO_2 equilibrium represented by Eq. 9, the currents which would be used experimentally to achieve reaction of both carbon species can be calculated from

values of ΔE between the voltage at which the reaction designated Eq. 29 will take place, up to the voltage at which electrolyte decomposition will occur (represented as Eq. 25 or 28). The applied current, I, is related to the voltage difference as follows:

$$I = -\Delta E \sigma \, A/l \, , \tag{33}$$

where σ is the conductivity of the ceramic electrolyte, and A/l is the ratio of the area to the thickness of the electrolyte. For matters of simplicity, this ratio was set equal to one. Values of σ for three different ceramic materials at temperatures of 1000, 1300, and 1500K were taken from data given by Sato (ref. 8). Since one mole of O_2 is produced when four equivalents of electrons combine with two moles of oxide ions, the rate of oxygen production is equal to $I/4F$. Table XI shows current and rate of oxygen production as E is varied, up to the voltage of cell decomposition. Figures 6-8 show graphs of applied voltage versus current, for three different ceramic electrolytes. Similar calculations can be performed for H_2O electrolysis. Due to the lower fugacity of water in the H_2-H_2O mixture, the applied voltage necessary to electrolyze water increases from the E values in Table X according to:

$$E = E_{(std)} - \frac{RT}{|z| F} \ln 1/f_{H_2O} \, , \tag{34}$$

where $E_{(std)}$ is the emf value at unit fugacity. At 1000K, the applied voltage increases from 1.00 to 1.15 v, and at 1500K, the change is from 0.85 to 0.93 v. The water fugacities used in these calculations are from Table VII. As water

is electrolyzed, the remaining gas becomes richer in hydrogen. This will not reduce the ceramic until f_{H_2}/f_{H_2O} equals 3.5×10^8 at 1500K, and equals 5.6×10^{13} at 1000K, however.

The results expressed in Table XI and shown in Figures 6-8 are for the production of oxygen at unit fugacity. The value of the electromotive force at any oxygen fugacity is

$$E = E_{(std)} - \frac{RT}{|z|} \frac{\nu}{F} \ln f_{O_2} , \qquad (35)$$

where ν is the stoichiometric coefficient of oxygen in Eqs. 25 through 31. Table XII shows the values of E, if oxygen were produced at its atmospheric partial pressure ($f_{O_2} = 0.21$) via the reactions represented by Eqs. 25 and 29. However the current for those reactions remains identical to the values given in Table XI. If plots of applied voltage versus current were to be made, they would be identical to those in Figures 6-8, except for a vertical displacement equal to the difference between E and $E_{(std)}$.

Finally, the product of voltage and current, EI, gives the ideal (non-thermal) power required to produce O_2. These power requirements are listed in Table XI for the various ceramics.

The rates of oxygen production given in Table XI are rather slow. However, one must remember that these values are for an electrolyte with an A/l ratio (v. Eq. 33) set equal to one. The commonly available ceramic tubes have an A/l ratio of somewhat greater than 100, thereby increasing the rate by at least two orders of magnitude.

CONCLUSIONS

The key conclusions of this study are:

- Thermodynamics indicate that the carbo-chlorination reaction for the reduction of anorthite occurs as described by Eq. 1.
- The effluent gases from carbo-chlorination and hydrogenation are essentially CO-CO_2 and H_2-H_2O, respectively.
- Volatilizable materials associated with lunar anorthite or ilmenite do not significantly alter the species present in the effluent gases, even when large amounts of O_2 are removed.
- Only Cl_2 from carbo-chlorination effluents has significant interactions with the proposed high temperature ceramic electrolytes, which suggests that some type of chlorine scrubber may have to be employed in this process.

Therefore, this study indicates that electrolysis of the refining gases from carbo-chlorination of anorthite and hydrogenation of ilmenite should be an effective means of oxygen production. Unfortunately, kinetic data for these reactions cannot be determined by calculations or from previous studies. Experimentation is necessary. Also, due to lack of knowledge of kinetic data and lack of knowledge of the effect of a platinum coating on the ceramic, it is not possible to tell if the decomposition of the electrolyte by chlorine will in actuality occur. If it does occur, it may be possible to alleviate this problem by simply passing the effluent gases through a CaO trap before allowing them to enter the cell. In such a case, the chlorine would be converted to $CaCl_2$, and calcium carbonate would <u>not</u> be formed, as the gases are above the temperature at which $CaCO_3$ decomposes to CaO and CO_2.

REFERENCES

1. D.R. Stull, H. Prophet, JANAF Thermochemical Tables, 2nd ed., U.S. Government Printing Office, Washington, 1971.
2. K.K. Kelley, Bureau of Mines Bulletin 584, 1960.
3. V.B. Parker, D.D. Wagman, W.H. Evans, NBS Technical Note 270-6, 1971.

4a. R.A. Robie, D.R. Waldbaum, Geological Survey Bulletin 1259, 1968.

b. R.A. Robie, B.S. Hemingway, J.R. Fisher, Geological Survey Bulletin 1452, 1978.

5. J. Weissbart, W.H. Smart, T. Wydeven, "Design and Performance of a Solid Electrolyte Oxygen Generator Test Module," Paper 71-Av-8, SAE/ASME/AIAA Life Support and Environmental Control Conference, San Francisco, July 12-14, 1971.
6. R.J. Williams, ed., Handbook of Lunar Materials, NASA-Johnson Space Center, 1978.
7. J.H. Canterford, R. Colton, Halides of the Second and Third Row Transition Metals, Wiley-Interscience, London, 1968.
8. M. Sato, in Research Techniques for High Pressure and High Temperature, G.C. Ulmer, ed., Springer-Verlag, New York, 1971.
9. P. Deines, R.F. Nafziger, G.C. Ulmer, E. Woermann, Bulletin of the Earth and Mineral Sciences Experimental Station, University Park, Pa., The Pennsylvania State University, No. 88, 1974.

Table I.– Possible reactions during carbo-chlorination

1) $CaAl_2Si_2O_8+Cl_2 \rightarrow CaCl_2+Al_2SiO_5+SiO_2+1/2\ O_2$

2) $3CaAl_2Si_2O_8+3Cl_2 \rightarrow 3CaCl_2+Al_6Si_2O_{13}+4SiO_2+3/2\ O_2$

3) $CaAl_2Si_2O_8+Cl_2 \rightarrow CaCl_2+Al_2O_3+2SiO_2+1/2\ O_2$

4) $1/2\ O_2+CaCl_2+SiO_2 \rightarrow CaSiO_3+Cl_2$

5) $O_2+2CaCl_2+SiO_2 \rightarrow Ca_2SiO_4+2Cl_2$

6) $3/2\ O_2+3CaCl_2+Al_2O_3 \rightarrow Ca_3Al_2O_6+3Cl_2$

7) $1/2\ O_2+CaCl_2+2Al_2O_3 \rightarrow CaAl_4O_7+Cl_2$

8) $1/2\ O_2+CaCl_2+Al_2O_3 \rightarrow CaAl_2O_4+Cl_2$

9) $6O_2+12CaCl_2+7Al_2O_3 \rightarrow Ca_{12}Al_{14}O_{33}+12\ Cl_2$

Table II.– Thermodynamic Data of Carbo-chlorination reactions at fixed f_{Cl_2} ; 1000K

Reaction*	ΔG(kJ)	K	f_{Cl_2}	f_{O_2}
1	+1.443	0.841	2.99×10^{-11}	6.33×10^{-22}
2	+14.142	0.182	2.99×10^{-11}	2.87×10^{-22}
3	+7.222	0.420	2.99×10^{-11}	1.58×10^{-22}
4	+21.451	7.58×10^{-2}	2.99×10^{-11}	1.56×10^{-19}
5	+86.454	3.05×10^{-5}	2.99×10^{-11}	2.93×10^{-17}
6	+263.923	1.63×10^{-14}	2.99×10^{-11}	1.39×10^{-12}
7	+55.911	1.19×10^{-3}	2.99×10^{-11}	6.31×10^{-16}
8	+57.262	1.02×10^{-3}	2.99×10^{-11}	8.59×10^{-16}
9	+893.912	2.01×10^{-47}	2.99×10^{-11}	5.42×10^{-14}

*Number refers to reaction listed in Table I.

Table III.— Thermodynamic Data of Carbo-chlorination Reactions at fixed f_{O_2}

a. 1000K

Reaction*	ΔG(kJ)	K	f_{O_2}	f_{Cl_2}
1	+1.443	0.841	6.33×10^{-22}	2.99×10^{-11}
2	+14.142	0.182	6.33×10^{-22}	4.44×10^{-11}
3	+7.222	0.420	6.33×10^{-22}	5.99×10^{-11}
4	+21.451	7.58×10^{-2}	6.33×10^{-22}	1.91×10^{-12}
5	+86.454	3.05×10^{-5}	6.33×10^{-22}	1.39×10^{-13}
6	+263.923	1.63×10^{-14}	6.33×10^{-22}	6.38×10^{-16}
7	+55.911	1.19×10^{-3}	6.33×10^{-22}	2.99×10^{-14}
8	+57.262	1.02×10^{-3}	6.33×10^{-22}	2.57×10^{-14}
9	+893.912	2.01×10^{-47}	6.33×10^{-22}	3.23×10^{-15}

b. 1100K

Reaction*	ΔG(kJ)	K	f_{O_2}	f_{Cl_2}
1	+6.602	0.486	1.00×10^{-20}	2.06×10^{-10}
2	+25.794	5.96×10^{-2}	1.00×10^{-20}	2.56×10^{-10}
3	+12.003	0.269	1.00×10^{-20}	3.72×10^{-10}
4	+18.820	0.128	1.00×10^{-20}	1.28×10^{-11}
5	+81.396	1.36×10^{-4}	1.00×10^{-20}	1.17×10^{-12}
6	+252.785	9.89×10^{-13}	1.00×10^{-20}	9.96×10^{-15}
7	+50.342	4.07×10^{-3}	1.00×10^{-20}	4.07×10^{-13}
8	+52.907	3.07×10^{-3}	1.00×10^{-20}	3.07×10^{-13}
9	+841.720	1.06×10^{-40}	1.00×10^{-20}	4.66×10^{-14}

*Number refers to reaction listed in Table I.

Table III.— Thermodynamic Data of Carbo-chlorination Reactions at fixed f_{O_2} — continued

c. 1200K

Reaction*	ΔG(kJ)	K	f_{O_2}	f_{Cl_2}
1	+10.247	0.358	1.58×10^{-19}	1.11×10^{-9}
2	+32.769	3.75×10^{-2}	1.58×10^{-19}	1.19×10^{-9}
3	+15.083	0.220	1.58×10^{-19}	1.81×10^{-9}
4	+17.707	0.170	1.58×10^{-19}	6.76×10^{-11}
5	+78.165	3.96×10^{-4}	1.58×10^{-19}	7.91×10^{-12}
6	+245.588	2.04×10^{-11}	1.58×10^{-19}	1.09×10^{-13}
7	+45.894	1.00×10^{-2}	1.58×10^{-19}	3.97×10^{-12}
8	+49.819	6.78×10^{-3}	1.58×10^{-19}	2.69×10^{-12}
9	+804.190	9.81×10^{-36}	1.58×10^{-19}	4.81×10^{-13}

d. 1300K

Reaction*	ΔG(kJ)	K	f_{O_2}	f_{Cl_2}
1	+13.544	0.286	6.30×10^{-19}	2.78×10^{-9}
2	+38.731	2.78×10^{-2}	6.31×10^{-19}	2.62×10^{-9}
3	+17.774	0.193	6.31×10^{-19}	4.12×10^{-9}
4	+16.954	0.208	6.31×10^{-19}	1.65×10^{-10}
5	+75.266	9.45×10^{-4}	6.31×10^{-19}	2.44×10^{-11}
6	+239.806	2.31×10^{-10}	6.31×10^{-19}	4.87×10^{-13}
7	+42.204	2.01×10^{-2}	6.31×10^{-19}	1.60×10^{-11}
8	+47.242	1.26×10^{-2}	6.31×10^{-19}	1.00×10^{-11}
9	+772.035	9.48×10^{-32}	6.31×10^{-19}	2.06×10^{-12}

*Number refers to reaction listed in Table I.

Table III.– Thermodynamic Data of Carbo-chlorination Reactions at fixed f_{O_2} – concluded

e. 1400K

Reaction*	ΔG(kJ)	K	f_{O_2}	f_{Cl_2}
1	+16.778	0.237	3.16×10^{-18}	7.50×10^{-9}
2	+44.572	2.17×10^{-2}	3.16×10^{-18}	6.37×10^{-9}
3	+20.384	0.174	3.16×10^{-18}	1.02×10^{-8}
4	+16.322	0.246	3.16×10^{-18}	4.37×10^{-10}
5	+72.626	1.95×10^{-3}	3.16×10^{-18}	7.85×10^{-11}
6	+234.756	1.74×10^{-9}	3.16×10^{-18}	2.14×10^{-12}
7	+38.710	3.59×10^{-2}	3.16×10^{-18}	6.38×10^{-11}
8	+44.949	2.10×10^{-2}	3.16×10^{-18}	3.73×10^{-11}
9	+742.267	2.01×10^{-28}	3.16×10^{-18}	8.75×10^{-12}

f. 1500K

Reaction*	ΔG(kJ)	K	f_{O_2}	f_{Cl_2}
1	+19.941	0.202	1.00×10^{-17}	1.57×10^{-8}
2	+50.262	1.78×10^{-2}	1.00×10^{-17}	1.21×10^{-8}
3	+22.920	0.159	1.00×10^{-17}	1.99×10^{-8}
4	+15.477	0.289	1.00×10^{-17}	9.14×10^{-10}
5	+70.367	3.54×10^{-3}	1.00×10^{-17}	1.88×10^{-10}
6	+231.865	8.42×10^{-9}	1.00×10^{-17}	6.43×10^{-12}
7	+35.221	5.93×10^{-2}	1.00×10^{-17}	1.88×10^{-10}
8	+42.589	3.29×10^{-2}	1.00×10^{-17}	1.04×10^{-10}
9	+701.740	3.64×10^{-25}	1.00×10^{-17}	2.91×10^{-11}

*Number refers to reaction listed in Table I.

Table IVa.— Composition of Beneficiated Anorthite

Species	%	moles/100.32g	moles relative to oxygen
SiO_2	44.90	.7473	1.4946
TiO_2	0.05	.0006	.0012
Al_2O_3	33.67	.3302	.9906
Cr_2O_3	0.01	.00006	.0002
FeO	1.09	.0152	.0152
MnO	0.01	.0001	.0001
MgO	1.35	.0335	.0335
CaO	18.59	.3315	.3315
Na_2O	0.45	.0073	.0073
K_2O	0.16	.0017	.0017
P_2O_5	0.03	.0002	.0010
S	0.01	.0003	—
Total	100.32	1.4680	2.8769

Table IVb.— Composition of Beneficiated Ilmenite

Species	%	moles of reactive oxygen/99.19g
SiO_2	3.78	—
TiO_2	48.10	—
Al_2O_3	1.07	—
Cr_2O_3	0.49	—
FeO	43.28	.6024
MnO	0.03	—
MgO	1.29	—
CaO	1.07	—
Na_2O	0.04	—
K_2O	0.01	—
P_2O_5	0.01	—
S	0.02	—
Total	99.19	.6024

Table IVc.— Volatile Substances in Lunar Material

Species	moles/100g anorthite or ilmenite
N	0.0100
H	0.0075
Ne	0.0001
He	0.0018
C	0.0100

Table V.— Effluent gases from carbo-chlorination, 1000K

a. 100% CO

Species	moles	mole fraction (X) = partial pressure
CO	2.8714	.996
H_2O	0.0038	.001
N_2	0.0050	.002
P_4O_{10}	0.0001	.00003
SO_2	0.0002	.00007
SO_3	0.0001	.00003
He+Ne	0.0019	.0006

b. "63.6% CO, 36.4% CO_2"

Species	moles	X
CO	1.3359	.632
CO_2	0.7678	.363
H_2O	0.0038	.002
N_2	0.0050	.002
P_4O_{10}	0.0001	.00005
SO_2	0.0002	.00009
SO_3	0.0001	.00005
He+Ne	0.0019	.001

Table VI.– Effluent gases from carbo-chlorination after disproportionation of CO. T = 1000K

a. $CO_2/CO = \infty$

Species	moles	X
CO_2	1.4357	.992
H_2O	0.0038	.003
N_2	0.0050	.003
P_4O_{10}	0.0001	.00007
SO_2	0.0002	.0001
SO_3	0.0001	.00007
He+Ne	0.0019	.001

b. $CO_2/CO = 100$

Species	moles	X
CO_2	1.4286	.983
CO	0.0143	.010
H_2O	0.0038	.003
N_2	0.0050	.003
P_4O_{10}	0.0001	.00007
SO_2	0.0002	.0001
SO_3	0.0001	.00007
He+Ne	0.0019	.001

c. $CO_2/CO = 10$

Species	moles	X
CO_2	1.3673	.902
CO	0.1367	.090
H_2O	0.0038	.003
N_2	0.0050	.003
P_4O_{10}	0.0001	.00007
SO_2	0.0002	.0001
SO_3	0.0001	.00007
He+Ne	0.0019	.001

Table VII.— Effluent gases from hydrogenation

a. T = 1000K

Species	moles	X
H_2	18.2835	.967
H_2O	0.5975	.031
CO	0.0043	.0002
CO_2	0.0002	.00001
CH_4	0.0055	.0003
N_2	0.0050	.0003
P_4O_6	0.00003	—
H_2S	0.0006	.00003
He+Ne	0.0019	.0001

b. T = 1500K

Species	moles	X
H_2	3.4934	.851
H_2O	0.5921	.144
CO	0.0099	.002
CO_2	0.0001	.00002
N_2	0.0050	.001
P_4O_6	0.00003	—
H_2S	0.0006	.0001
He+Ne	0.0019	.0005

Table VIII.— Effluent gases from carbo-chlorination, 1000K

a. following 90% electrolysis

Species	moles	X
CH_4	0.0003	.001
H_2	0.0028	.011
H_2O	0.0001	.0004
CO	0.1854	.744
CO_2	0.0533	.214
N_2	0.0050	.020
P_4O_6	0.0001	.0004
H_2S	0.0003	.001
He+Ne	0.0019	.008

b. following 99% electrolysis

Species	moles	X
CH_4	0.0003	.008
H_2	0.0028	.074
H_2O	0.0001	.003
CO	0.0213	.560
CO_2	0.0062	.163
N_2	0.0050	.132
P_4O_6	0.0001	.003
H_2S	0.0003	.008
He+Ne	0.0019	.050

Table IX.– Effluent gases from hydrogenation

a. following 90% electrolysis, 1000K

Species	moles	X
H_2	18.8130	.996
H_2O	0.0598	.003
CO	0.0004	.00002
CH_4	0.0096	.0005
N_2	0.0050	.0003
P_4O_6	0.00003	—
H_2S	0.0006	.00003
He+Ne	0.0019	.0001

b. following 99% electrolysis, 1000K

Species	moles	X
H_2	18.8660	.999
H_2O	0.0060	.0003
CH_4	0.0100	.0005
N_2	0.0050	.0003
P_4O_6	0.00003	—
H_2S	0.0006	.00003
He+Ne	0.0019	.0001

Table IX.– Effluent gases from hydrogenation – concluded

c. following 90% electrolysis, 1500K

Species	moles	X
H_2	4.0215	.983
H_2O	0.0592	.014
CO	0.0010	.0002
CH_4	0.0024	.0006
N_2	0.0050	.001
P_4O_6	0.00003	—
H_2S	0.0006	.0001
He+Ne	0.0019	.0005

d. following 99% electrolysis, 1500K

Species	moles	X
H_2	4.0746	.996
H_2O	0.0059	.001
CO	0.0001	—
CH_4	0.0025	.0006
N_2	0.0050	.001
P_4O_6	0.00003	—
H_2S	0.0006	.0001
He+Ne	0.0019	.0005

Table X.— Emf of electrolysis reactions; $f_{O_2} = 1$

a. $ZrO_2 \rightarrow Zr+O_2$

T(K)	ΔG(kJ)	E (v)
1000	+907.083	-2.35
1100	+888.640	-2.30
1200	+870.063	-2.25
1300	+851.427	-2.21
1400	+832.863	-2.16
1500	+814.462	-2.11

b. $CO_2 \rightarrow CO+1/2\ O_2$

T(K)	ΔG(kJ)	E (v)
1000	+195.681	-1.01
1100	+187.007	-0.97
1200	+178.372	-0.92
1300	+169.766	-0.88
1400	+161.197	-0.84
1500	+152.662	-0.79

c. $CO \rightarrow C+1/2\ O_2$

T(K)	ΔG(kJ)	E (v)
1000	+200.242	-1.04
1100	+209.041	-1.08
1200	+217.773	-1.13
1300	+226.463	-1.17
1400	+235.095	-1.22
1500	+243.680	-1.26

Table X.— Emf of electrolysis reactions; $f_{O_2} = 1$ — continued

d. $CaO \rightarrow Ca+1/2\ O_2$

T(K)	ΔG(kJ)	E (v)
1000	+532.083	-2.76
1100	+521.845	-2.70
1200	+511.000	-2.65
1300	+499.946	-2.59
1400	+489.080	-2.53
1500	+478.156	-2.48

e. $H_2O \rightarrow H_2+1/2\ O_2$

T(K)	ΔG(kJ)	E (v)
1000	+192.559	-1.00
1100	+186.989	-0.97
1200	+181.374	-0.94
1300	+175.730	-0.91
1400	+170.040	-0.88
1500	+164.322	-0.85

f. $ThO_2 \rightarrow Th+O_2$

T(K)	ΔG(kJ)	E (v)
1000	+1037.519	-2.69
1100	+1019.206	-2.64
1200	+1000.876	-2.59
1300	+ 982.638	-2.55
1400	+ 964.125	-2.50
1500	+ 946.333	-2.45

Table X.– Emf of electrolysis reactions; $f_{O_2} = 1$ – concluded

g. $Y_2O_3 \rightarrow 2Y+3/2\ O_2$

T(K)	ΔG(kJ)	E (v)
1000	+1614.512	-2.79
1100	+1586.474	-2.74
1200	+1558.536	-2.69
1300	+1530.709	-2.64
1400	+1503.007	-2.60
1500	+1475.356	-2.55

Table XI.– Current and Rates of Oxygen Production of CO_2 electrolysis; A/l = 1

a. 13% CaO stabilized ZrO_2; 1000K, log σ = -2.5

ΔE (v)	I (amp)	Rate (mol/sec)	Power (watts)
0	0	0	0
-0.50	1.58×10^{-3}	4.09×10^{-9}	2.39×10^{-3}
-1.00	3.16×10^{-3}	8.19×10^{-9}	6.35×10^{-3}
-1.34	4.24×10^{-3}	1.10×10^{-8}	9.96×10^{-3}

b. 13% CaO stabilized ZrO_2; 1300K, log σ = -1.3

ΔE (v)	I (amp)	Rate (mol/sec)	Power (watts)
0	0	0	0
-0.50	2.51×10^{-2}	6.49×10^{-8}	3.46×10^{-2}
-1.00	5.01×10^{-2}	1.30×10^{-7}	9.42×10^{-2}
-1.33	6.67×10^{-2}	1.73×10^{-7}	1.47×10^{-1}

c. 13% CaO stabilized ZrO_2; 1500K, log σ = -0.7

ΔE (v)	I (amp)	Rate (mol/sec)	Power (watts)
0	0	0	0
-0.50	9.98×10^{-2}	2.58×10^{-7}	1.29×10^{-1}
-1.00	2.00×10^{-1}	5.17×10^{-7}	3.58×10^{-1}
-1.32	2.63×10^{-1}	6.82×10^{-7}	5.55×10^{-1}

d. 10% Y_2O_3 stabilized ZrO_2; 1000K, log σ = -1.9

ΔE (v)	I (amp)	Rate (mol/sec)	Power (watts)
0	0	0	0
-0.50	6.29×10^{-3}	1.63×10^{-8}	9.50×10^{-3}
-1.00	1.26×10^{-2}	3.26×10^{-8}	2.53×10^{-2}
-1.34	1.69×10^{-2}	4.38×10^{-8}	3.97×10^{-2}

Table XI.– Current and Rates of Oxygen Production of CO_2 electrolysis; A/l = 1 – continued

e. 10% Y_2O_3 stabilized ZrO_2; 1300K, log σ = -0.9

ΔE (v)	I (amp)	Rate (mol/sec)	Power (watts)
0	0	0	0
-0.50	6.29×10^{-2}	1.63×10^{-7}	8.68×10^{-2}
-1.00	1.26×10^{-1}	3.26×10^{-7}	2.37×10^{-1}
-1.33	1.67×10^{-1}	4.34×10^{-7}	3.69×10^{-1}

f. 10% Y_2O_3 stabilized ZrO_2; 1500K, log σ = -0.55

ΔE (v)	I (amp)	Rate (mol/sec)	Power (watts)
0	0	0	0
-0.50	1.41×10^{-1}	3.65×10^{-7}	1.82×10^{-1}
-1.00	2.82×10^{-1}	7.31×10^{-7}	5.05×10^{-1}
-1.32	3.72×10^{-1}	9.64×10^{-7}	7.85×10^{-1}

g. 2.5% Y_2O_3 stabilized ThO_2; 1000K, log σ = -3.05

ΔE (v)	I (amp)	Rate (mol/sec)	Power (watts)
0	0	0	0
-0.50	4.46×10^{-4}	1.16×10^{-9}	6.73×10^{-4}
-1.00	8.91×10^{-4}	2.31×10^{-9}	1.79×10^{-3}
-1.30	1.16×10^{-3}	3.01×10^{-9}	2.68×10^{-3}
-1.68	1.50×10^{-3}	3.88×10^{-9}	4.04×10^{-3}

h. 2.5% Y_2O_3 stabilized ThO_2; 1300K, log σ = -1.9

ΔE (v)	I (amp)	Rate (mol/sec)	Power (watts)
0	0	0	0
-0.50	6.29×10^{-3}	1.63×10^{-8}	8.68×10^{-3}
-1.00	1.26×10^{-2}	3.26×10^{-8}	2.37×10^{-2}
-1.30	1.64×10^{-2}	4.24×10^{-8}	3.58×10^{-2}
-1.67	2.10×10^{-2}	5.45×10^{-8}	5.36×10^{-2}

Table XI.– Current and Rates of Oxygen Production of CO_2 electrolysis; $A/l = 1$ – concluded

1. 2.5% Y_2O_3 stabilized ThO_2; 1500K, log σ = -1.3

ΔE (v)	I (amp)	Rate (mol/sec)	Power (watts)
0	0	0	0
-0.50	2.51×10^{-2}	6.50×10^{-8}	3.24×10^{-2}
-1.00	5.01×10^{-2}	1.30×10^{-7}	8.97×10^{-2}
-1.30	6.52×10^{-2}	1.69×10^{-7}	1.36×10^{-1}
-1.66	8.32×10^{-2}	2.16×10^{-7}	2.04×10^{-1}

Table XII.— Emf of electrolysis reactions; $f_{O_2} = 0.21$

a. $ZrO_2 \rightarrow Zr+O_2$

T(K)	E (std) (v)	E (v)
1000	-2.35	-2.32
1100	-2.30	-2.26
1200	-2.25	-2.21
1300	-2.21	-2.17
1400	-2.16	-2.11
1500	-2.11	-2.06

b. $CO_2 \rightarrow CO+1/2\ O_2$

T(K)	E (std) (v)	E (v)
1000	-1.01	-0.98
1100	-0.97	-0.93
1200	-0.92	-0.88
1300	-0.88	-0.84
1400	-0.84	-0.79
1500	-0.79	-0.74

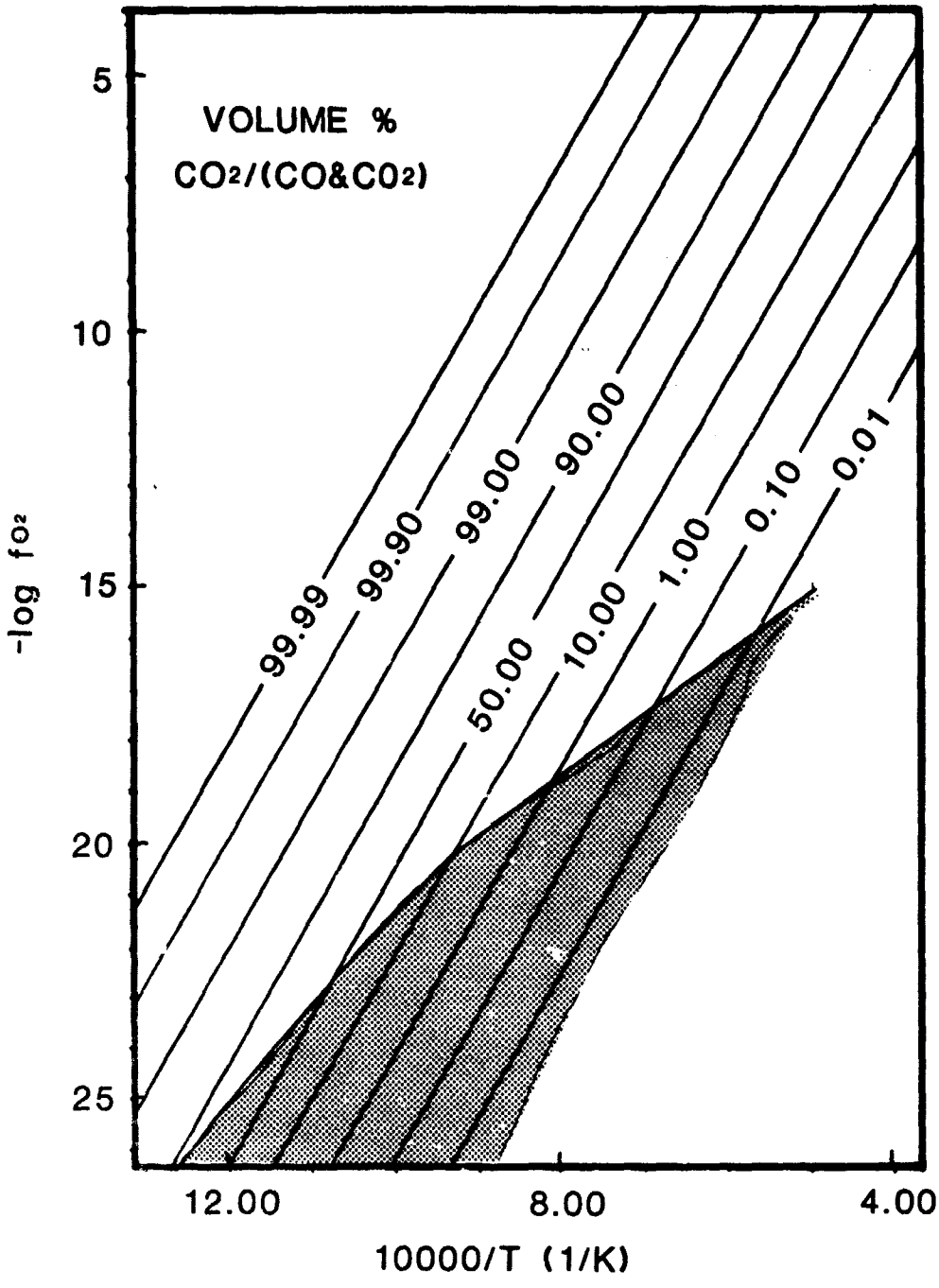

Figure 1.- Volume percent isopleths summarizing f_{O_2}-T calculations for CO-CO_2 mixtures. Shaded area is prohibited by precipitation of carbon (and is, therefore, the minimum f_{O_2} for that temperature). Total pressure is 1.01325×10^5 Pa (1 atm.) (ref. 9).

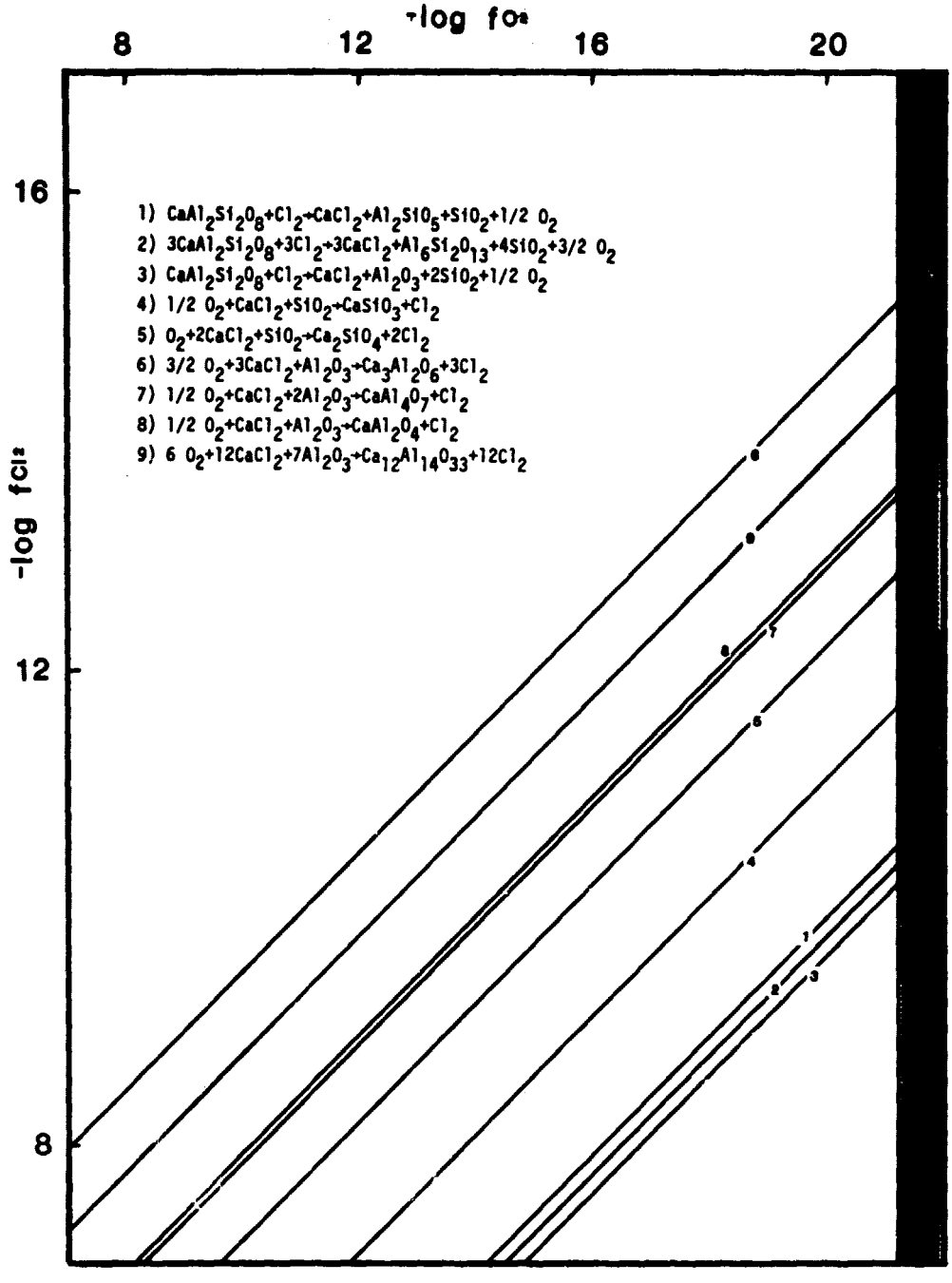

Figure 2.- The effect of f_{O_2} and f_{Cl_2} on which of the various carbo-chlorination reactions can occur. Shaded area indicates the f_{O_2} minimum due to carbon precipitation. Total pressure is 10^5 Pa (1 bar), temperature is 1000K.

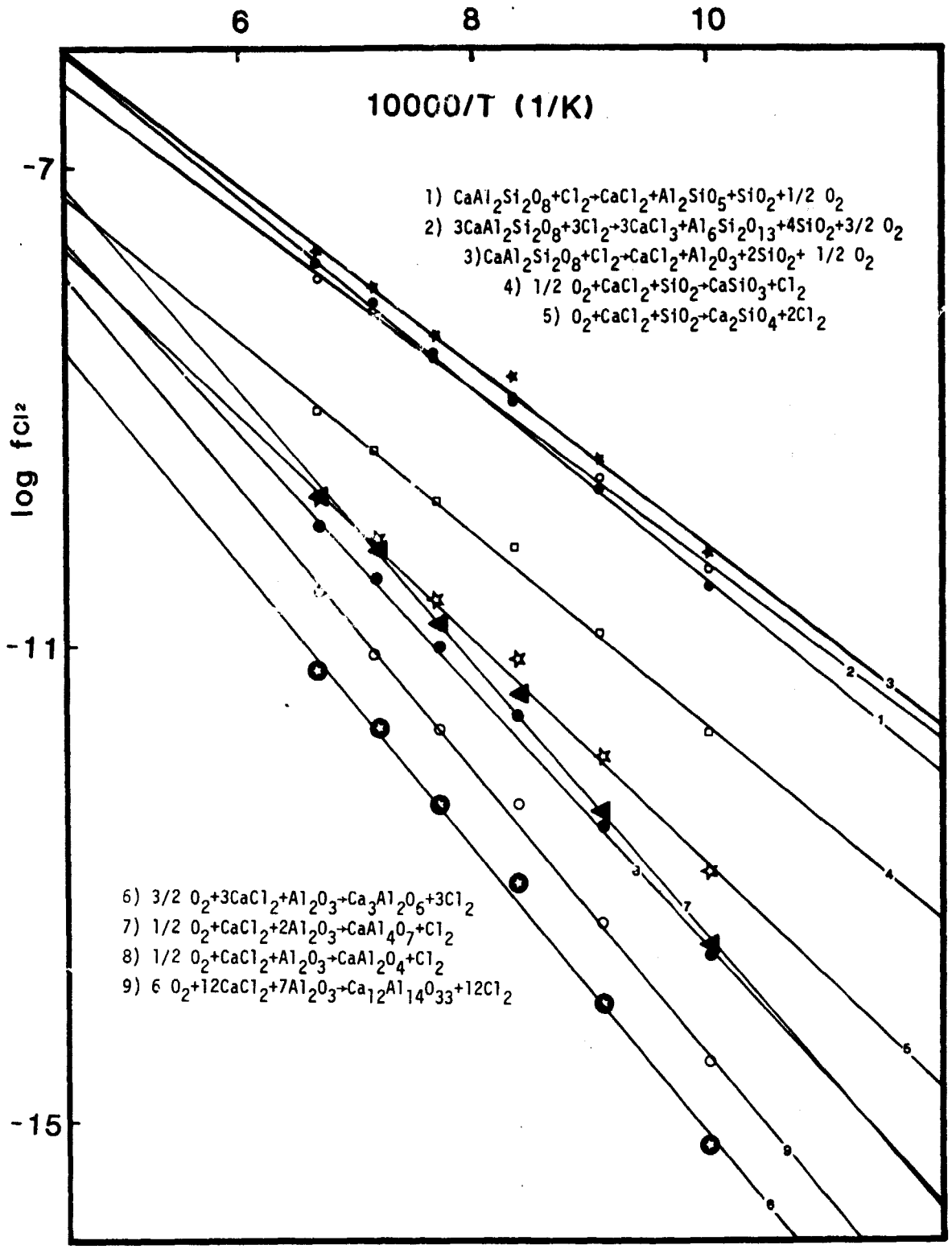

Figure 3.- The effect of f_{Cl_2} and T on the various carbo-chlorination reactions, at minimum f_{O_2}. Total pressure is 10^5 Pa (1 bar).

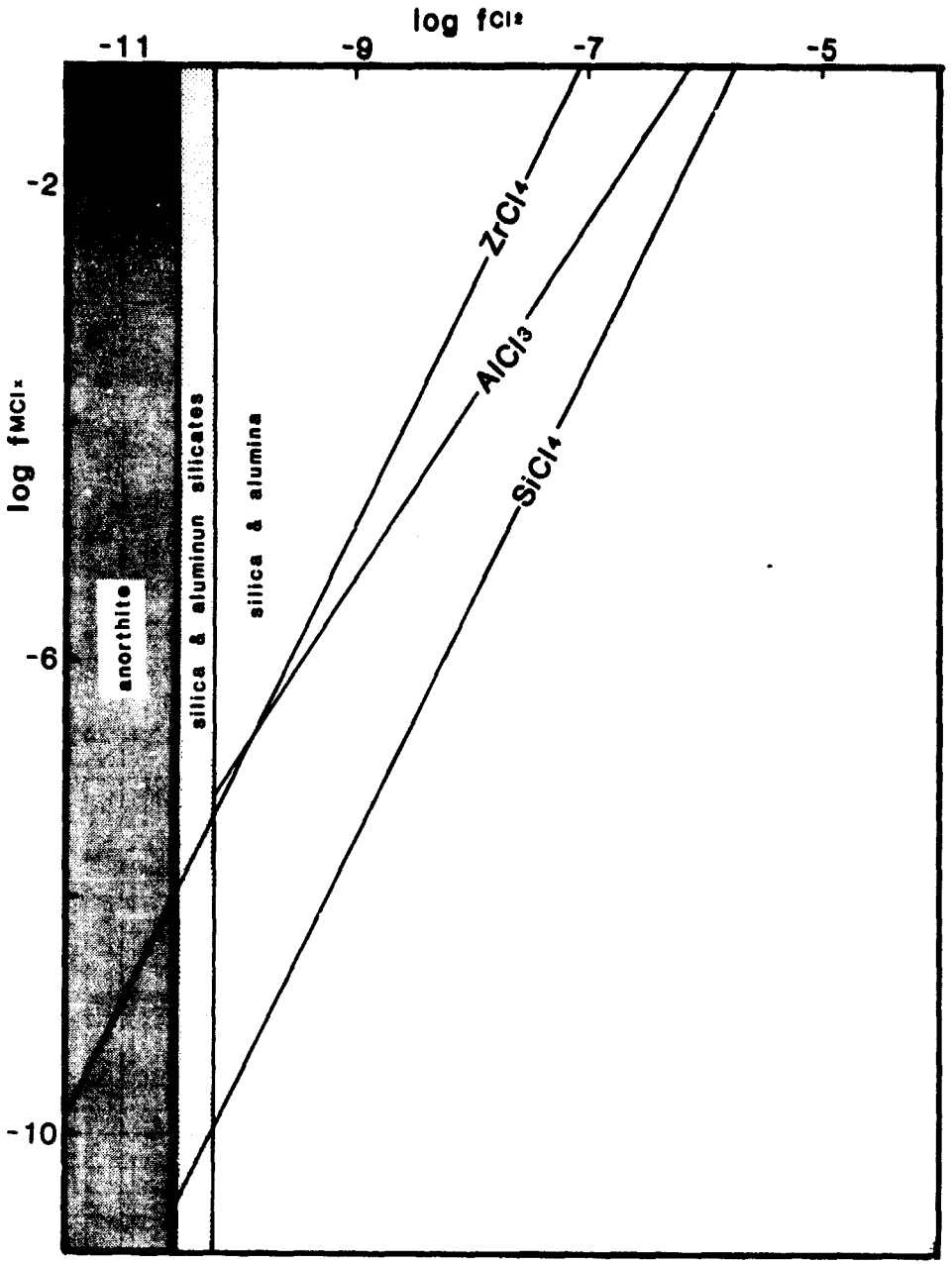

Figure 4.- Extent of production of gaseous metal chlorides as a function of f_{Cl_2}, at minimum f_{O_2}. Region of anorthite stability implies that neither $SiCl_4$ nor $AlCl_3$ can be formed. Region of silica-aluminum silicate stability implies that $SiCl_4$, but not $AlCl_3$, can be formed. Total pressure is 10^5 Pa (1 bar), temperature is 1000K.

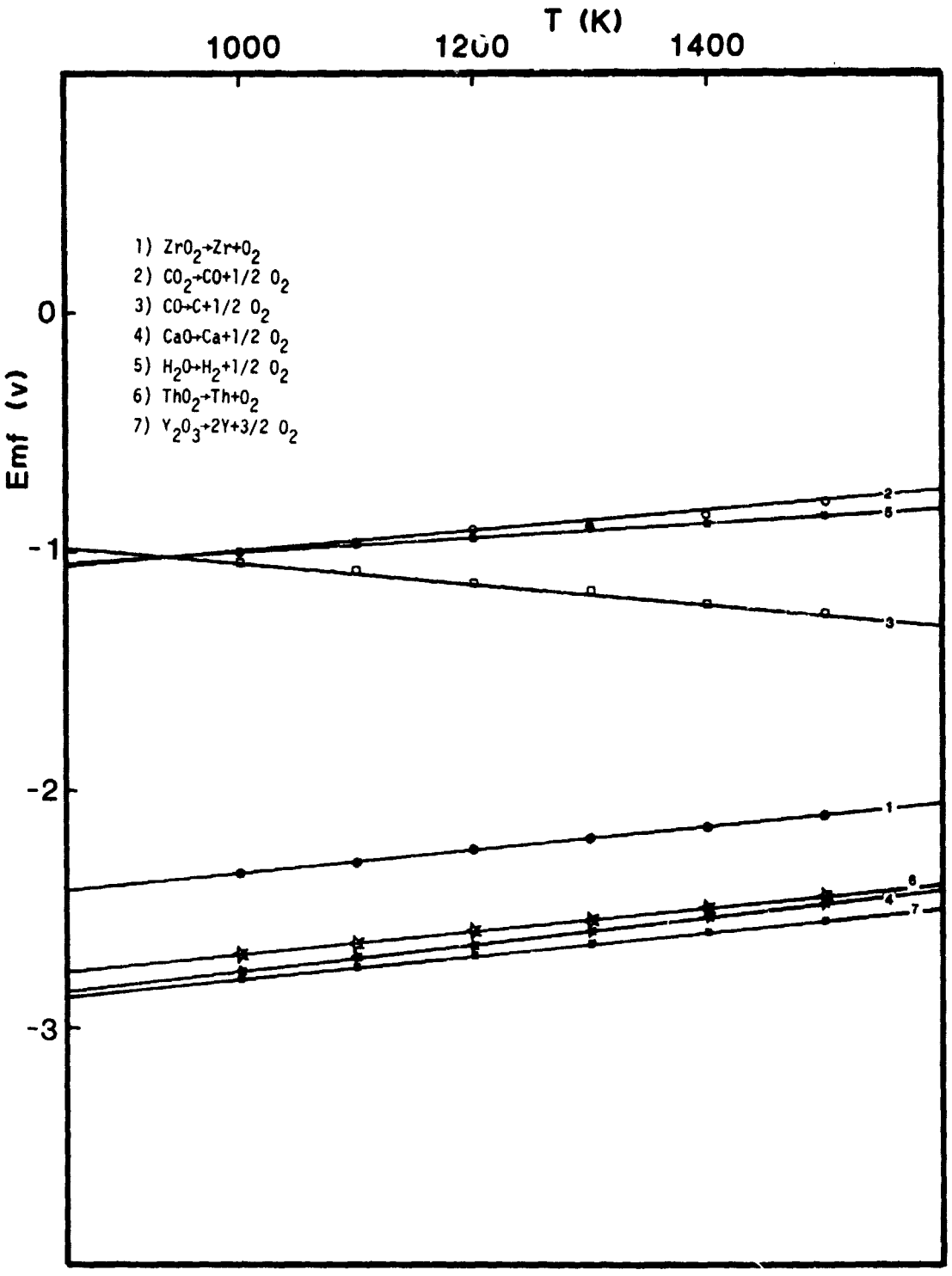

Figure 5.- The effect of temperature on electromotive force for oxide reduction. Pressure of effluent oxygen is 10^5 Pa (1 bar).

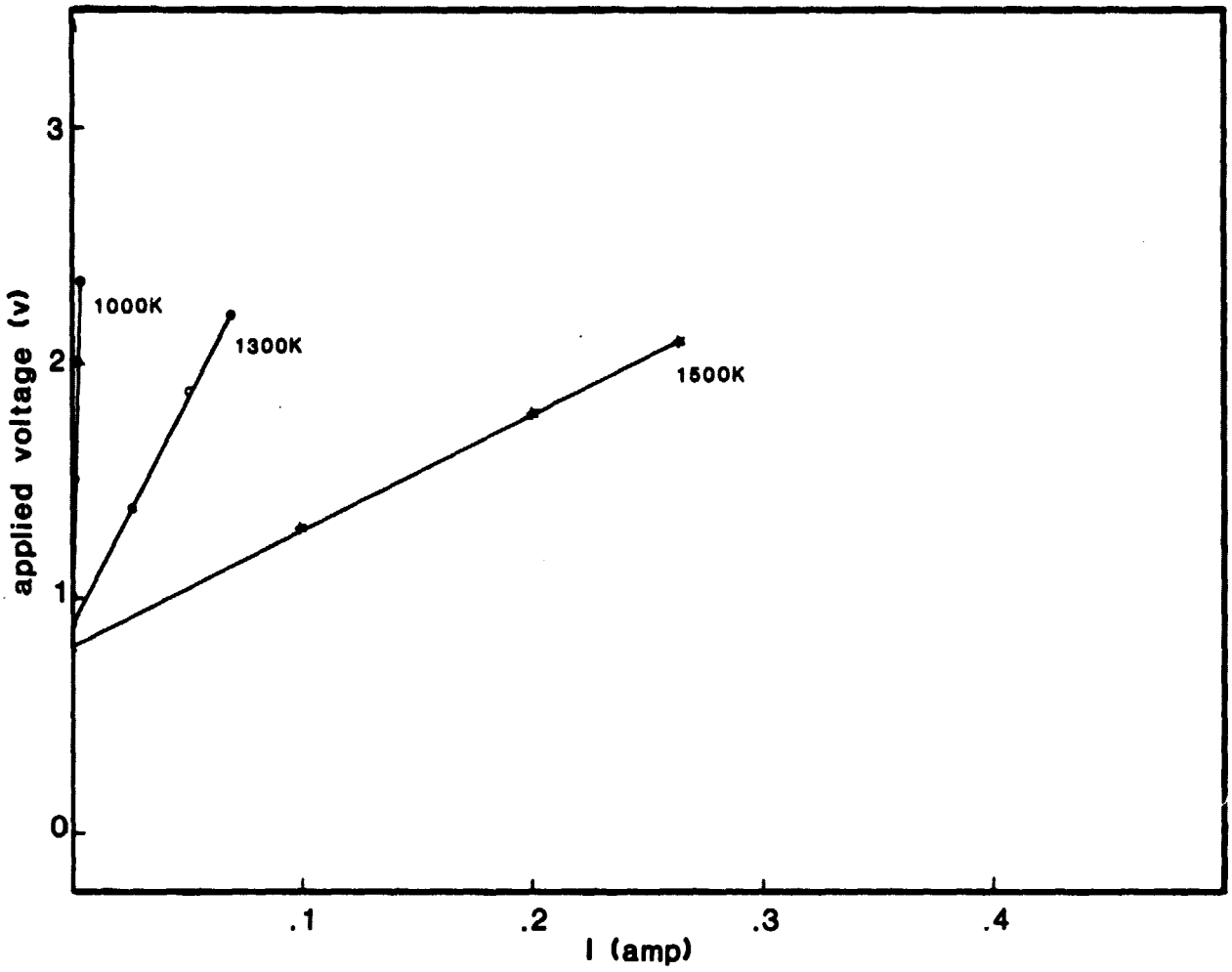

Figure 6.- Applied voltage versus current for the electrolysis of CO_2 using a 13% calcia stabilized zirconia electrolyte, up to the decomposition voltage of the ceramic. Calculations performed for three temperatures. Pressure of effluent oxygen is 10^5 Pa (1 bar).

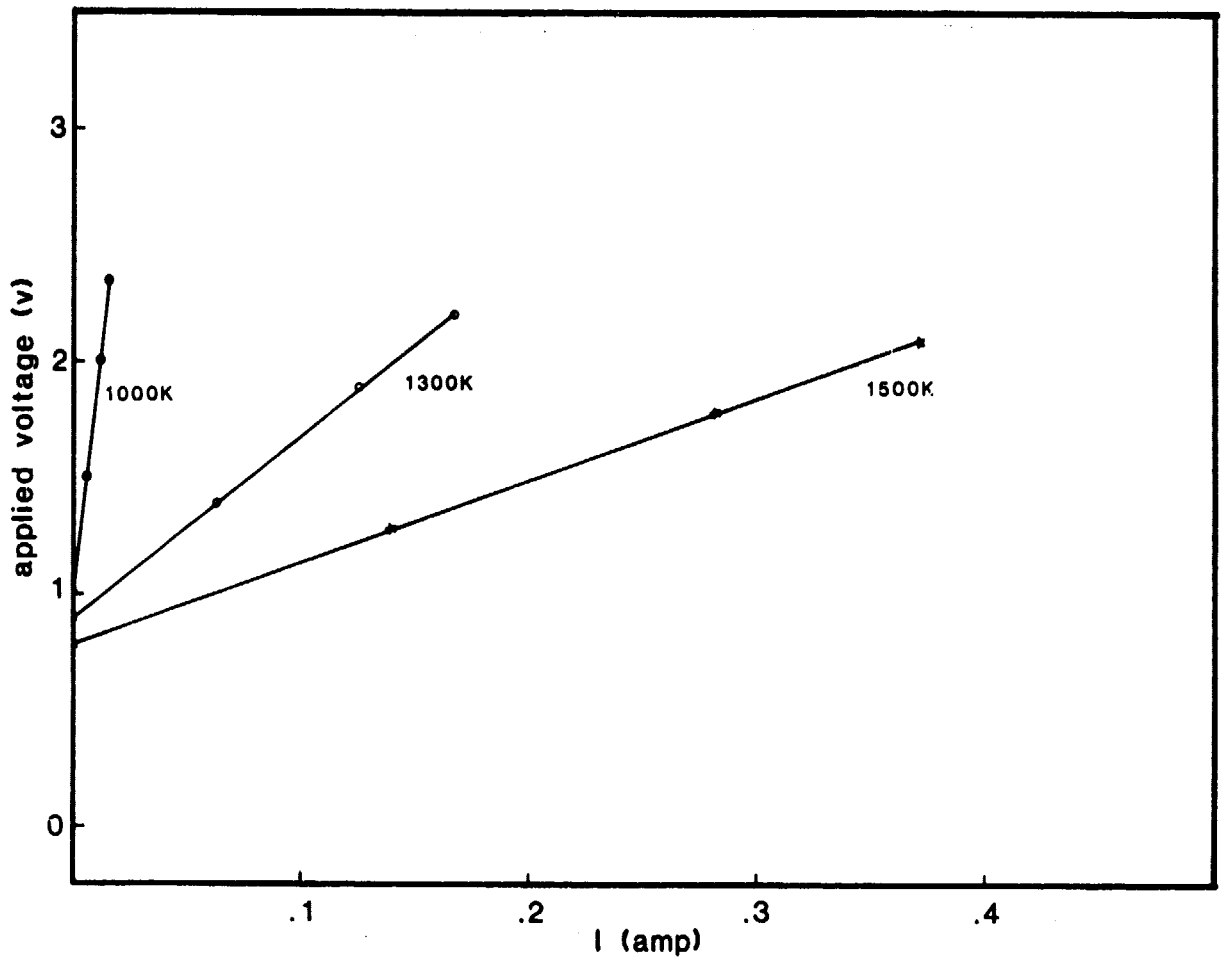

Figure 7.- Applied voltage versus current for the electrolysis of CO_2 using a 10% yttria stabilized zirconia electrolyte, up to the decomposition voltage of the ceramic. Calculations performed for three temperatures. Pressure of effluent oxygen is 10^5 Pa (1 bar).

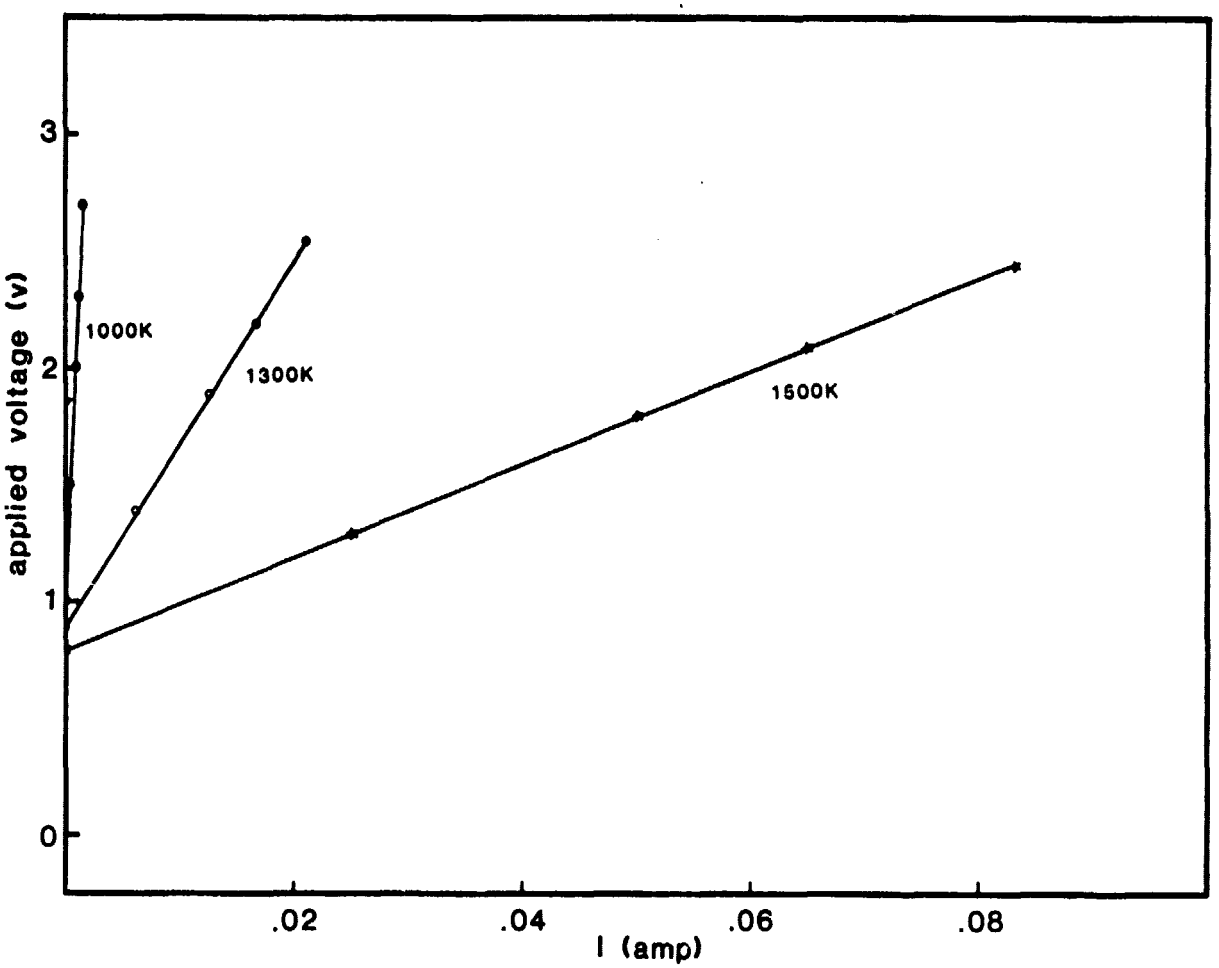

Figure 8.- Applied voltage versus current for the electrolysis of CO_2 using a 2.5% yttria stabilized thoria electrolyte, up to the decomposition voltage of the ceramic. Calculations performed for three temperatures. Pressure of effluent oxygen is 10^5 Pa (1 bar).